Journal of Advanced Research 52 (2023) 89–102

Contents lists available at ScienceDirect

Journal of Advanced Research

journal homepage: www.elsevier.com/locate/jare

Original Article

Live and pasteurized *Akkermansia muciniphila* decrease susceptibility to *Salmonella* Typhimurium infection in mice

Jiaxiu Liu, Hongli Liu, Huanhuan Liu, Yue Teng, Ningbo Qin, Xiaomeng Ren, Xiaodong Xia *

National Engineering Research Center of Seafood, School of Food Science and Technology, Dalian Polytechnic University, Dalian, Liaoning 116034, China

HIGHLIGHTS

- Pretreatment with AKK or pAKK modulates *S.* Typhimurium infection.
- AKK enhances the gut barrier and increases RegIII lectins secretion after infection.
- pAKK stimulates antimicrobial activity, ROS production, and inflammasome activation in macrophages and mice.
- AKK-altered gut microbiota plays a partial role in attenuating infection.

GRAPHICAL ABSTRACT

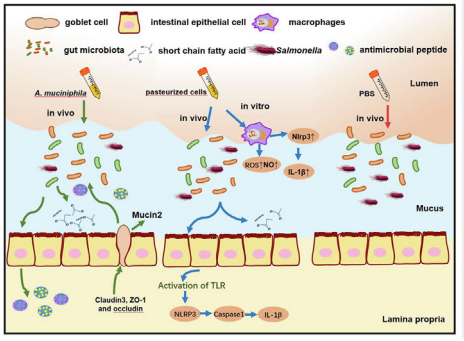

ARTICLE INFO

Article history:
Received 15 November 2022
Revised 2 March 2023
Accepted 23 March 2023
Available online 28 March 2023

Keywords:
Akkermansia muciniphila
Salmonella Typhimurium
Gut microbiota
RegIII lectins
Gut barriers
Inflammasomes

ABSTRACT

Introduction: The gut microbiome is vital for providing resistance against colonized pathogenic bacteria. Recently, specific commensal species have become recognized as important mediators of host defense against microbial infection by a variety of mechanisms.
Objectives: To examine the contribution of live and pasteurized *A. muciniphila* to defend against the intestinal pathogen *Salmonella* Typhimurium in a streptomycin-treated mouse model of infection.
Methods: C57B6J mice were pretreated with phosphate-buffered saline (PBS), live *Akkermansia muciniphila* (AKK), and pasteurized *A. muciniphila* (pAKK) for two weeks, then mice were infected by *S.* Typhimurium SL 1344. 16S rRNA-based gut microbiota analysis was performed before and after infection. Bacterial counts in feces and tissues, histopathological analysis, gut barrier-related gene expression, and antimicrobial peptides were examined. Co-housing was performed to examine the role of microbiota in the change of susceptibility of mice to infection.
Results: AKK and pAKK markedly decreased *Salmonella* fecal and systemic burdens and reduced inflammation during infection. Notably, further characterization of AKK and pAKK protective mechanisms revealed different candidate protective pathways. AKK promoted gut barrier gene expression and the secretion of antimicrobial peptides, and co-housing studies suggested that AKK-associated microbial community played a role in attenuating infection. Moreover, pAKK had a positive effect on NLRP3 in infected mice. We verified that pretreatment of pAKK could promote the expression of NLRP3, and enhance the antimicrobial activity of macrophage, likely through increasing the production of reactive oxygen (ROS), nitric oxide (NO), and inflammatory cytokines.

* Corresponding author.
E-mail address: foodscixiaodong@dlpu.edu.cn (X. Xia).

https://doi.org/10.1016/j.jare.2023.03.008

Conclusion: Our study demonstrates that live or pasteurized *A. muciniphila* can be effective preventive measures for alleviating *S.* Typhimurium-induced disease, highlighting the potential of developing Akkermansia-based probiotics or postbiotics for the prevention of Salmonellosis.

Introduction

Nontyphoidal *Salmonella enterica* subsp. *enterica* serovars is one of human intracellular bacterial pathogens responsible for hundreds of thousands of cases of acute gastroenteritis each year [1]. The infection cycle of the model nontyphoidal *S. enterica* serovar Typhimurium (*S.* Typhimurium) involves the consumption of contaminated food by a susceptible mammalian host (including humans and rodents), followed by acute intestinal inflammation [2]. The mucosal immune response to *S.* Typhimurium infection is complex and has been recently recognized to include activating the inflammasome resulting in the secretion of pro-inflammatory and anti-inflammatory factors [3]. The most thoroughly studied inflammasome is the nod-like receptor family, Pyrin Domain Containing 3 (NLRP3) inflammasome, which is crucial for host defense against a variety of infections, including bacteria [4,5], viruses [6], and protozoan parasites [7].

Gut microbiota colonized in the mammalian gastrointestinal (GI) tract is an enormous community of microbes that extensively interact with the intestinal immune system [8]. Host resistance to enteric infection relies largely on the protective effects of the resident gut microbiome through niche competition, antagonistic metabolite production, or activation of host immunity to secret antimicrobial peptides, which is known as 'colonization Resistance' (CR) [8,9]. The microbiota and its output metabolites are essential components for the regulation or activation of host intestinal immunity against bacterial pathogens through indirect, direct, or both mechanisms [9-11]. Numerous studies have shown that some commensal-metabolized metabolites produced by intestinal microorganisms protect mice against infection, such as bile acids against *Clostridium difficile* [12], SCFAs produced by *Bacteroides* species against *S.* Typhimurium, *Klebsiella pneumonia*, and *Escherichia coli* [13], and antigen A produced by *Enterococcus faecium* against *S.* Typhimurium [14]. Meanwhile, intestinal microbiome members can affect the function of mammalian intestinal epithelial cells or immune cells by improving the expression of antimicrobial peptides (AMPs) or ROS production [10]. These findings have emphasized the importance of commensal bacteria to the host immune function and control of enteric pathogenesis.

A. muciniphila is a gram-negative, mucin-degrading anaerobe bacterium, which has been increasingly recognized as a key mediator of human health [15]. Since the discovery of *A. muciniphila*, an increasing number of studies have shown strong associations between *A. muciniphila* and metabolic disorders, such as obesity, glucose metabolism, as well as intestinal immune functions [16-19]. The potential mechanisms of action of *A. muciniphila* on health include regulation of gut microbiota, improvement of tight junctions, and reduction of inflammation. Meanwhile, specific cell components or secreted substances from *A. muciniphila* contributing to its beneficial effects have been identified, such as Amuc_1100 [20], Amuc_2109 [21], Amuc_2172 [22], Protein 9 (P9)[23], and diacyl phosphatidylethanolamine (PE) [24]. These substances may explain the recent findings which demonstrated that pasteurized *A. muciniphila* also exhibited positive effects on host health, sometimes being even more efficient than live bacterium [20].

Although *A. muciniphila* (either live or pasteurized) has been extensively examined for its role in chronic disorders such as obesity, diabetes, and cancer, the influences of AKK (especially pasteurized AKK) on enteric infectious diseases have been rarely explored. One previous study in 2013 has shown that *A. muciniphila* exacerbated inflammation induced by *S.* Typhimurium in gnotobiotic mice supplied with simplified human intestinal microbiota (SIHUMI) [25]. In contrast, one recent study has reported that *A. muciniphila* provides a protective effect against infection induced by *Citrobacter rodentium* [26]. These studies indicated that *A. muciniphila* might be involved in intestinal bacterial pathogens infection.

In this study, we used a mouse model of salmonellosis to dissect the effects of live or pasteurized *A. muciniphila* on *S.* Typhimurium infection. Live *A. muciniphila* administration reduced bacterial burdens *in vivo* in a manner potentially related to the enhanced gut barrier function and increased secretion of antimicrobial lectins. In contrast, while pasteurized *A. muciniphila* administration also ameliorated *S.* Typhimurium infection outcomes, we found that this phenotype could be due to inflammasome activation, which initiates innate immune responses, such as the activation of NLRP3 pathway. Our findings suggest protective mechanisms for live and pasteurized *A. muciniphila* in *S.* Typhimurium pathogenesis and provide insights into the pathways by which intestinal commensals interact with both host and pathogen.

Materials and Methods

Ethics statement

All experimental procedures were performed according to the Guide for Laboratory Animals of the National Institute of Health. It was approved by the Animal Ethics Committee of Dalian Polytechnic University (No DLPU2020004).

Animals

Six to eight-week-old male C57BL/6J mice (Specified pathogen-free, SPF) were purchased from Changsheng (Liaoning, China) and mice were maintained in SPF controlled environment (12 h day light on and 12 h lights off, 24 ± 1 °C).

Salmonella strains

Salmonella enterica serovar Typhimurium strains used in this study are streptomycin-resistant derivative of SL1344 strain, which were purchased from the American Type Culture Collection (ATCC). *S.* Typhimurium strains SL1344 harboring (green fluorescent protein) GFP plasmid was from our laboratory collection. Two strains were cultured overnight at 37 °C before use.

Culturing of A. muciniphila and preparation of pasteurized A. muciniphila (pAKK)

A. muciniphila (ATTC BAA-835) was cultured in a basal mucin-based medium under an anaerobic chamber as previously described [27]. *A. muciniphila* was cultured overnight at 37 °C under strictly anaerobic conditions and stored at −80 °C. pAKK was prepared as previously described [20]. Briefly, grown *A. muciniphila* was centrifuged at 12,000 *g* for 10 min to remove media, rinsed twice and suspended in 0.01 M PBS, and pasteurized for

30 min at 70 °C. Before use, *A. muciniphila* and pAKK were diluted with 0.01 M PBS to a concentration of 2×10^8 CFU/200 μL.

Cell culture

Macrophages RAW 264.7 were purchased from the Cell Bank of the Chinese Academy of Sciences (Shanghai, China). RAW 264.7 was cultured in Dulbecco's Modified Eagle Medium (DMEM, Gibco, USA) containing 10% (v/v) fetal bovine serum (FBS, Hyclone, USA) and 1% (v/v) double antibiotic solution (100 U/mL penicillin and 100 μg/mL streptomycin, Hyclone, USA) at 37 °C and 5% CO_2.

Gentamicin protection assay

Macrophages RAW 264.7 were prepared as described in cell culture seeded at the plate, and incubated at 37 °C and 5% CO_2 for 18 h. RAW 264.7 cells were pretreated with 1 μg/ml of LPS (Sigma, USA), or with AKK and pAKK, both at the multiplicity of infection (MOI) of 10 for 24 h. Then RAW 264.7 cells were infected for 45 min with *S.* Typhimurium followed by gentamicin treatment for 1 h at 37 °C. Macrophages RAW 264.7 lysed in 0.1% (v/v) triton buffer, and the lysate was plated on LB agar plates supplemented with 100 μg/mL of streptomycin (SM). For further research, RAW 264.7 were exposed to 20 μM of NLRP3 inhibitor MCC950 (MCE, USA) for 24 h before the treatment of pasteurized AKK for another 24 h.

S. Typhimurium infection model

Before infection, *S.* Typhimurium strains SL1344 was cultured overnight in LB medium containing streptomycin. Mice were orally gavaged with streptomycin (SM) with a dose of 25 mg/mouse 24 h in advance before infection. Then, mice were infected with 10^7 CFU/100 μL of *S.* Typhimurium SL1344 by oral gavage. Mice were distinguished by tail markings, and weight was tracked daily throughout the whole test. At each time point, 2–3 fresh fecal pellets were collected into sterile tubes, weighed, and homogenized in 1 mL 0.01 M PBS by a Mini-Beadbeater (BioSpec, USA). Fecal *Salmonella* burdens were determined by plating serial dilutions on selective Xylose Lysine Desoxycholate (XLD) plates containing 200 μg/mL streptomycin.

Mice were euthanized and tissues were collected using sterile dissection tools. Bacterial loads in the spleen, liver, mesenteric lymph nodes (MLN), small intestine (SI), colon, and contents were determined as described as bacteria burdens in feces.

ELISA analysis

The levels of cytokines were measured by ELISA Kits according to the manufacturer's instructions, including IL-6, IL-1β, IL-10, TNFα, and IFN-γ (Jiancheng, China), or lipocalin-2 and D-Lactate (Mlbio, China).

Histological analysis

Samples of the cecal tissues were collected and fixed in a 4% (v/v) paraformaldehyde (PFA) solution to assess the severity of the infection. Tissue sections were mounted on glass slides and stained with hematoxylin and eosin (H&E) for histologic evaluation using previously published criteria [14]. Each tissue section was microscopically assessed for the extent of submucosal edema, preservation of epithelial integrity, and goblet cell retention, as well as for polymorphonuclear cell infiltration into the lamina propria (each category scored from 0 to 4). The overall scores represent the combined pathological score reported for each sample. There are three levels of inflammation: severe inflammation (scores $\geq$ 12), moderate Inflammation (scores of 8 to 12), mild inflammation (scores of 4 to 8), and no inflammation (scores $\leq$ 4).

Immunofluorescence staining

For immunofluorescence microscopy, the cecal section was fixed with 4% PFA, then dehydrated with the gradients of ethanol. The cecal section was permeabilized in PBS with 0.1 % (v/v) of Tween 20 before being washed in an immunostaining washing solution (Beyotime Biotechnology, China) and blocked for 1 h with immunostaining blocking solution. Then, the cecal section was incubated with primary antibodies overnight at 4 °C. The information of primary antibodies was listed as follows: rabbit anti-Mucin 2 (1:250; Proteintech, China), rabbit anti-ZO-1 (1:250; Abclonal, China), rabbit polyclonal anti-Claudin3 (1:500; Proteintech, China), and rabbit polyclonal anti-Occludin (1:250; Proteintech, China). After incubation, the cecal section was washed by washing solution 3 times, then incubated with secondary antibodies. The Alexa Fluor 488 (1:500; Beyotime Biotechnology, China) was used for Mucin 2 and ZO-1 staining, and Alexa Fluor 647 (1:500; Beyotime Biotechnology, China) was used for Claudin3 and Occludin. Cell nuclei were stained with DAPI. Images were visualized using fluorescence microscopy (Eclipse Ti-E, Nikon, Japan).

Immunoblotting

For protein extraction, cecum tissue was homogenized by bead beating in RIPA buffer (Beyotime Biotechnology, China). Then the concentration of proteins was tested by BCA Protein Assay Kit (Solarbio, China), then the protein was diluted to 1 mg/ml using SDS-PAGE loading buffer (Solarbio, China).

For SDS-PAGE, the sample loading volume is 10 μL per well, then separated by Bolt 10% and 12% Bis-Tris Gel (Beyotime Biotechnology, China) at a constant voltage (90 V) for 120 min respectively. Then the sample was transferred to nitrocellulose membranes (Life Technologies, USA) in ice at a constant current 300 mA for 90 min. The nitrocellulose membranes were incubated with primary antibodies overnight at 4 °C. The information of primary antibodies was listed as follows: rabbit polyclonal anti-Mucin 2 (1:1000; Proteintech, China), rabbit polyclonal anti-ZO1 (1:1000; Abclonal, China), rabbit polyclonal anti-Occludin (1:1000; Proteintech, China), rabbit polyclonal anti-Claudin3 (1:5000; Proteintech, China), rabbit polyclonal anti-TLR4 (1:1000; Abclonal, China), rabbit polyclonal anti-NLRP3 (1:1000; Abclonal, China), rabbit polyclonal anti-Caspase-1 (1:1000; Abcam, USA), rabbit polyclonal anti-IL-1β (1:1000; CST, USA), rabbit polyclonal anti-iNOS (1:1000; Abclonal), mouse polyclonal anti- Reg3β (1;1:1000; R&D, USA), rabbit polyclonal anti- Reg3γ (1:1000; Abclonal, China), and mouse or rabbits monoclonal anti-β-actin (1:2000, Beyotime, China) for overnight. After incubation, membranes were probed with secondary antibodies. The information of primary antibodies was listed as follows: mouse monoclonal anti-β-actin (1:2000, Beyotime Biotechnology, China) or rabbit monoclonal anti-β-actin (1:2000, Beyotime Biotechnology, China) for 1 h at room temperature. The band was detected by a Gel Imaging System (Bio-Rad, USA) and was quantified by ImageJ software.

Microbiota analysis

Fecal samples were collected after treatment and stored at −80 °C until analysis. Total bacterial DNA was isolated from fecal samples in mice using the E.Z.N.A.® soil DNA Kit (Omega Bio-Tek, U.S.) according to the protocol of the manufacturer. The hypervariable V3-V4 region of the microbial 16S rRNA gene was amplified by PCR using primers 338F 5′- ACTCCTACGGGAGGCAGCAG-3′ and 806R 5′-GGACTACHVGGGTWTCTAAT-3′. Sequencing was

performed using the Illumina MiSeq platform (Majorbio Biopharm, China). Closed reference operational taxonomic units (OTUs) were picked at 97% sequence similarity using the Research database (version 7.1 https://drive5.com/uparse/) and aligned with SILVA128/16S bacteria database for taxonomy information. The sequencing data were analyzed on the free online platform of Majorbio I-Sanger Cloud Platform (https://www.majorbio.com/).

Fecal SCFA quantification

SCFA measurements and qualification were performed as described previously [28]. 100 mg of feces were homogenized with 30 μL of 0.1 mol/L dilute sulphuric acid, 3 μL of internal standard solution (2-methyl butyric acid), and 1 mL of diethyl ether by Mini-Beadbeater (BioSpec, America) for the 40 s. After centrifugation at 12,000 *g* for 15 min, the fecal supernatant was collected. Then the supernatant was centrifuged at 12,000 *g* for 15 min with 250 mg sodium carbonate again, and filtered by 0.22 μm membranes (Millipore, USA) for use. SCFAs analysis was determined by Agilent (Agilent, Japan) 7890/5975 single quadrupole GC–MS with VF-WAXms capillary column (30 m × 25 mm × 0.25 μm). 0.1 μL of samples were injected into GC–MS and Helium was the carrier gas at 1 mL/min. The inlet temperature was 260 °C and the initial temperature of GC was 80 °C, ramped at 40 °C /min to 120 °C, then ramped at 10 °C /min to 200 °C and held for 2 min; total run time was 15 min. The mass spectrometer used electron ionization (70 eV) and the scan range was *m*/*z* 30–300 with a 2.5 min solvent delay. Standard curves were generated by linear regression. Unknown concentrations in samples were determined by the peak area integration of each SCFAs based on standard curves.

RNA isolation and gene expression

Cecal tissue samples were homogenized by bead beating in Trizol (Sangon, China) to extract RNA. cDNA was synthesized from extracted RNA with the PrimeScript™ Reverse Transcriptase Kit (Takara, Japan). Quantitative PCR assays were performed with a CFX Connect real-time PCR detection system (Bio-rad, USA) using the TB Green® Premix DimerEraser™ Kit (Takara, Japan). Relative gene expression was quantified by the $2^{-\triangle\triangle ct}$ method against the endogenous control GAPDH. The primers used for real-time PCR were acquired from Sangon and are listed in Table S1.

ROS and NO assay

RAW264.7 macrophages were seeded and grown in 96-well plates. After cell adherence, macrophages were pretreated with 1 μg/ml of LPS (Sigma, USA), or AKK, and pAKK at MOI of 10 for 24 h in DMEM without FBS, then infected with *S.* Typhimurium at MOI of 10 for 3 h. ROS and NO were detected before or after the infection.

Annexin v staining

Cell apoptosis was performed by the Annexin V staining kit (Beyotime, China) as the manufacturer's protocol. RAW 264.7 cells were pretreated by pAKK at MOI of 10 for 24 h, then infected by *Salmonella* at MOI of 10 for 3 h before staining.

Statistical analysis

All data presented in this study are expressed as mean ± standard error of the means (SEM). Statistical analyses were carried out by SPSS 23.0. Statistical significance was determined by one-way analysis of variance (ANOVA) or Kruskal-Wallis test for multiple comparisons, and post-hoc Tukey test or Mann-Whitney test for comparisons between two groups. Origin 2019b was used to draw all figures. The values $^{*}p < 0.05$, $^{**}p < 0.01$, and $^{***}p < 0.001$ were considered statistically significant.

Results

Effect of AKK and pAKK on intestinal gene expression, microbial community composition, and SCFA production before the infection

We first determined the effect of live and pasteurized AKK on intestinal gene expression and microbiota composition in mice before infection. Mice were orally gavaged with 0.01 M PBS, live or pasteurized of *A. muciniphila* once a day for two weeks. Administration of AKK or pAKK led to a slight reduction in normal body weight gain (Fig. 1A). Colon length showed similar length after treatment compared to control (Fig. 1B). Next, we examined the potential effect of AKK and pAKK on the expression of genes associated with gut barrier function. Significantly higher levels of expression of genes were detected in AKK-treated mice than AKK- or PBS-treated mice, including *Muc2* (Mucin2), *Tjp1* (ZO-1), *Ocln* (Occludin), and *Cldn3* (Claudin3) in Fig. 1 D-G. We also examined the expression of the antimicrobial RegIII lectins, which showed no significant difference among the three groups (Fig. 1H and I). Both AKK and pAKK increased SCFAs production in feces, especially acetic acid and propionic acid (Fig. 1J).

Then we examined the gut microbiota in each group of mice using 16S rRNA sequencing. Shannon index was markedly increased in AKK-treated mice in comparison with control (Fig. 1K). Principal coordinate analysis (PCoA) showed clear sample clustering of the AKK, pAKK, and PBS groups, indicating divergent community composition across three groups (Fig. 1L). Through the analysis of community composition, we found *Bacteroidetes* and *Firmicutes* were the dominant phyla in all mice, while pAKK-treated mice exhibited higher *Bacteroidetes* and lower *Firmicutes* relative abundances than the other two groups (Fig. 1M and N). The ratio of *Firmicutes* to *Bacteroidetes* was lower in pAKK-treated mice than that in other groups (Fig. 1O). Meanwhile, we noted that *Prevotellaceae*, *Bacteroidaceae*, and *Tannerellaceae* were richer in pAKK-treated mice, and *Bifidobacteriaceae* and *Erysipelotrichaceae* were richer in AKK-treated mice (Fig. 1P). By using *Akkermansia*-specific primers, we showed that AKK supplementation increased the fecal level of *A. muciniphila* about two-fold compared to control mice (Fig. S1). Collectively, these results indicate oral supplementation of AKK or pAKK could influence intestinal barrier gene expression and modify gut microbiota composition.

Pretreatment with AKK or pAKK modulates S. Typhimurium infection.

To determine whether AKK and pAKK pretreatment can protect mice from *S.* Typhimurium infection, we used a streptomycin-treated oral model of *S.* Typhimurium intestinal infection. All mice were pretreated with streptomycin for 24 h to enhance pathogen colonization, and subsequently orally challenged with *S.* Typhimurium SL1344 once (Fig. 2A). AKK or pAKK-pretreated mice were overall less susceptible to *S.* Typhimurium infection, as body weight loss in these two groups was higher than that in PBS group (Fig. 2B). Gross examination of organs from infected mice revealed reduced splenomegaly in AKK and pAKK-treated mice, whereas kidney and liver masses unchanged (Fig. S2A-C). Fecal *S.* Typhimurium loads were consistently lower throughout the infection in mice pretreated with AKK or pAKK than that in mice pretreated with PBS (Fig. 2C).

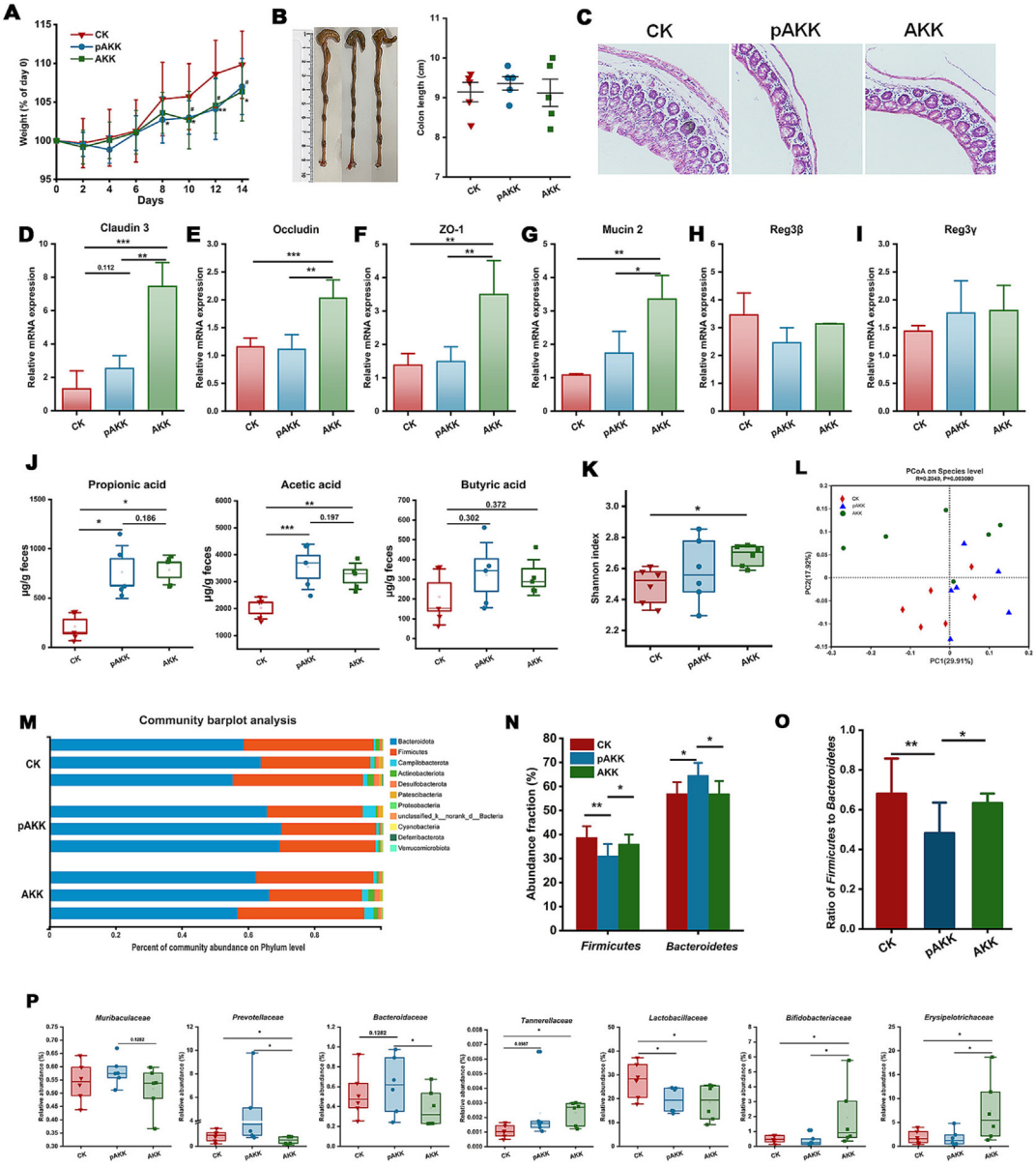

Fig. 1. AKK and pAKK treatment impacted tight junction protein expression, SCFA production, and gut microbial community composition in mice before infection. C57BL/6 mice were orally gavaged with PBS (CK). Live *A. muciniphila* (AKK) or pasteurized *A. muciniphila* (pAKK) for 14 days and euthanized on day 14. (A) Weight change. (B) Representatives image of colon (left) and colon length (right). (C) Representative H&E stained cecal sections of mice. Images were taken at × 10 magnification. The mRNA expression of (D) *Cldn3* (Claudin3), (E) *Ocln* (Occludin), (F) *Tjp1* (ZO-1), (G) *Muc2* (Mucin2), (H) *Reg3b*, and (I) *Reg3g*. (J) Quantification of SCFAs derived from fecal contents. (K-R) Microbial communities. (K) Shannon index and (L) PCoA analysis were shown. Each dot represented an individual in each group. (M) Relative abundance of bacterial phyla in three representative animals per group. (N) Boxplots displaying the relative abundance fractions of *Bacteroidetes* and *Firmicutes*; (O) The ratio of *Firmicutes* to *Bacteroidetes*; (P) The difference in the bacterial family among three groups. A-J: n = 5, K-P: n = 6. Statistical significance was determined by ANOVA or Kruskal-Wallis test for multiple comparisons, and post-hoc Tukey test or Mann-Whitney test for comparisons between two groups. *, $^{\#}p < 0.05$, **, $^{\#\#}p < 0.01$, and ***, $^{\#\#\#}p < 0.001$.

After infection, mice pretreated with AKK or pAKK also harbored significantly lower *S.* Typhimurium loads in extra-intestinal tissues, such as the spleen, liver, kidney, MLN, and intra-intestinal compartments, including the intestinal lumen and colon (Fig. 2D-K). Significant difference in colon length was observed after infection among all groups. Colons of AKK- or pAKK-pretreated mice were longer than mice pretreated with PBS (Fig. 2L). H&E staining displayed that AKK or pAKK treatment markedly reduced inflammation compared to control (Fig. 2M). AKK-pretreated mice exhibited an increased number of cecal goblet cells, suggesting AKK might have a positive effect on goblet cells (Fig. 2N). We further probed the host response in each group by profiling cytokine production in serum after infection (Fig. S2F-H). The enhanced levels of cytokines (IL-1β, IL-6, IL-10, and IFN-γ) in PBS-treated mice reflected the increased systemic *Salmonella* colonization in control group. Together, these results suggest that both AKK and pAKK modulate the outcome and host response to *Salmonella*-induced acute colitis.

Gut microbial community dynamics are altered by SM treatment in AKK and pAKK-treated mice

After SM treatment, previously observed differences in Shannon index were lost (Fig. 3A). PCoA showed the microbiota were more similar among three groups compared to the situation before infection (Fig. 3B). Phylum-level analysis revealed

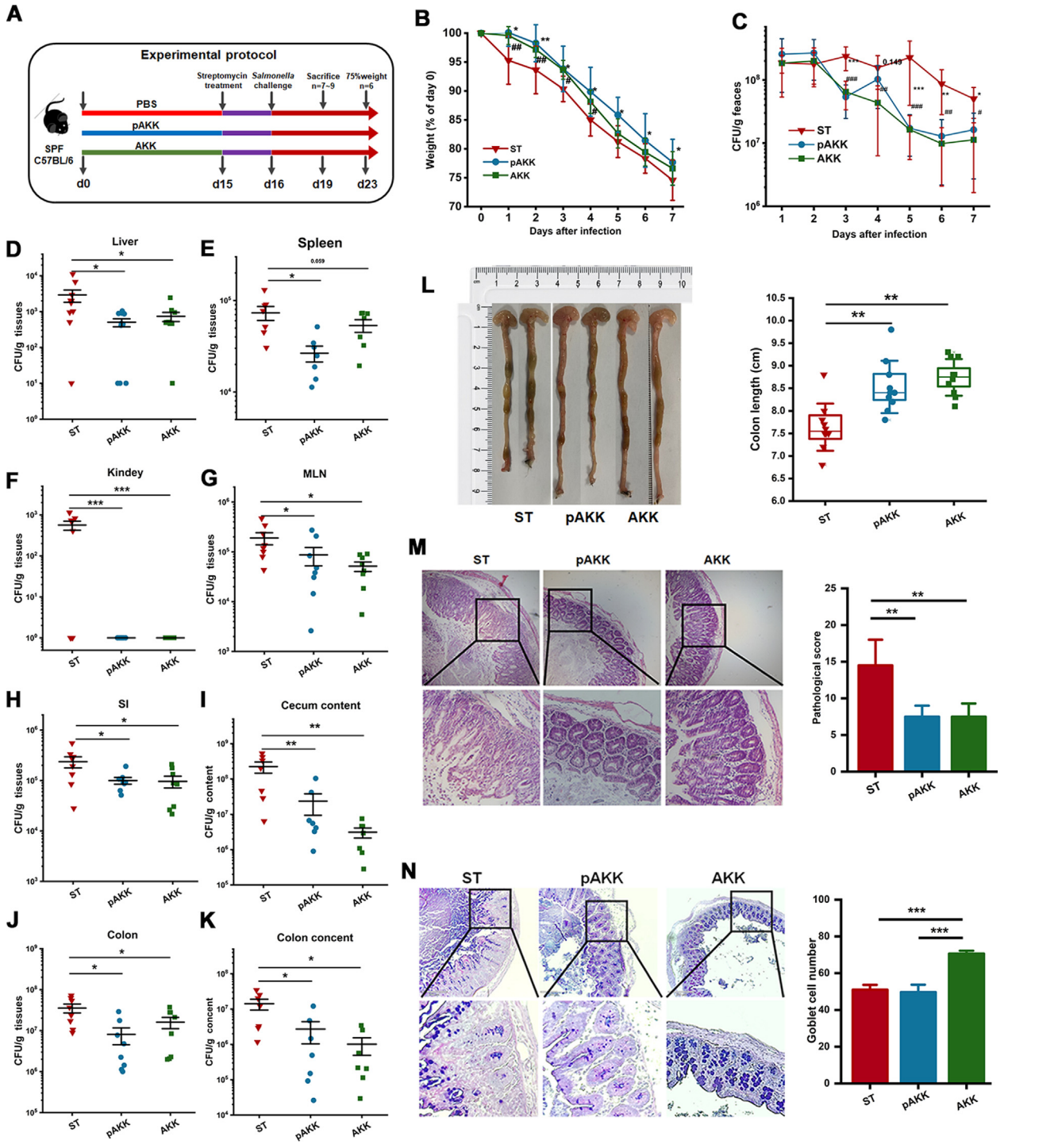

Fig. 2. AKK and pAKK treatment alleviated *S.* Typhimurium infection in mice. (A) Experimental design. After the 14-day intervention, C57BL/6 mice were orally gavaged with streptomycin, then challenged with 10^7 CFU/100 μL of *S.* Typhimurium SL1344. Here are two parts of the experiment. One part of the mice was sacrificed on day 23 for monitoring the trend of weight change and fecal shedding of pathogens, and the other part of the mice was sacrificed on day 19 for the determination of organ and tissue bacterial burdens and histopathology analysis. (B) Weight loss and (C) *S.* Typhimurium shedding in feces. *S.* Typhimurium burdens in tissues or intestinal contents, including (D) liver, (E) spleen, (F) kidney, (G) MLN, (H) SI, (I) cecal content, (J) colon, and (K) colon content. (L) Representative image of colon (left) and colon length (right). (M) Representative H&E stained cecal sections of mice (left) and associated histopathological scores after infection (right). Images were taken at × 10 magnification. (N) AB/PAS stained cecal sections of mice (left) and the number of goblet cells per crypt (right). Images were taken at × 10 magnification. B-C: n = 6, D-N: n = 7 ~ 10. Statistical significance was determined by ANOVA or Kruskal-Wallis test for multiple comparisons, and post-hoc Tukey test or Mann-Whitney test for comparisons between two groups. $^{*}p < 0.05$, $^{**}p < 0.01$, and $^{***}p < 0.001$.

Firmicutes and *Actinobacteria* as the dominant taxa, whereas the proportion of *Bacteroidetes* was obviously reduced in all mice after SM treatment (Fig. 3C and D), which was consistent with the previous study which showed significant *Bacteroidetes* reduction after streptomycin treatment [29]. Interestingly, despite the overall drop, *Bacteroidetes* in AKK-pretreated mice were more abundant (4.07%) than that in pAKK (0.28%) and SM group (0.36%) (Fig. 3E).

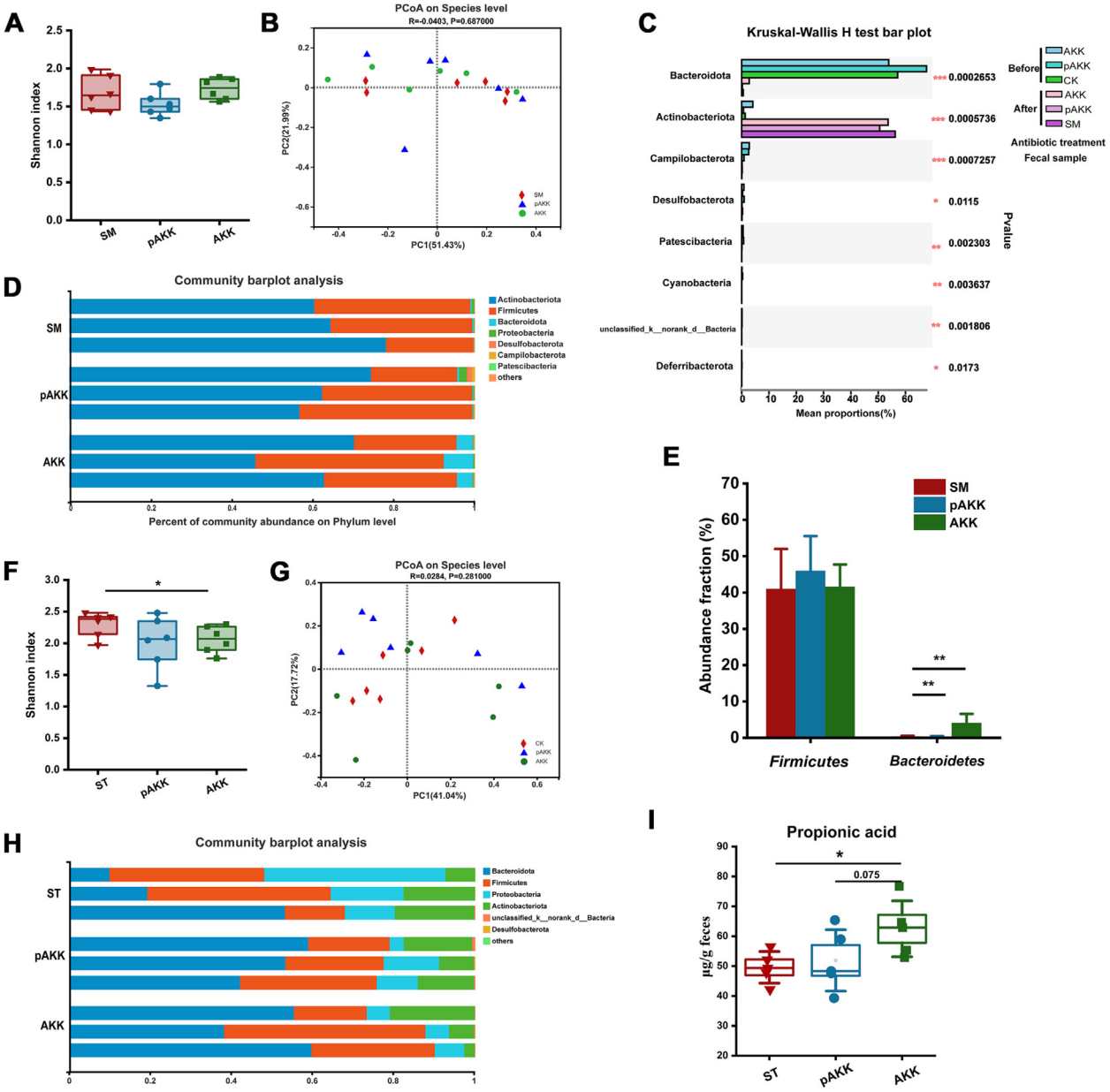

Fig. 3. AKK and pAKK modulated gut microbial community composition in the streptomycin-treated *S.* Typhimurium infection mice model. (A) Shannon index and (B) PCoA analysis were shown. Each dot represented an individual in each group. (C) Differences in microbial taxa before and after treatment of streptomycin. (D) Relative abundance of bacterial phyla in three representative animals per group. (E) Relative abundance of *Bacteroidetes* and *Firmicutes*. (F) Shannon index and (G) PCoA analysis were shown. Each dot represented an individual in each group. (H) Relative abundance of bacterial phyla in three representative animals per group. (I) Quantification of fecal propionic acid. A-H: n = 6, I: n = 5. Statistical significance was determined by ANOVA or Kruskal-Wallis test for multiple comparisons, and post-hoc Tukey test or Mann-Whitney test for comparisons between two groups. $^{*}p < 0.05$, $^{**}p < 0.01$, and $^{***}p < 0.001$.

Then, we analyzed the gut microbiota from *S.* Typhimurium-infected mice. We found a significant difference in the Shanon index among groups, and PCoA showed the microbiota were still similar after infection (Fig. 3F and G). *Bacteroidetes*, *Firmicutes*, *Proteobacteria*, and *Actinobacteria* were predominant in all infected mice (Fig. 3 H). *Bacteroidetes* produce SCFAs like propionate that prevents *S.* Typhimurium colonization [28]. Therefore we quantified SCFAs levels in AKK and pAKK-treated mice, and found higher levels of propionate in AKK-treated, compared to pAKK-treated or control mice (Fig. 3I), while no difference was observed for other SCFAs (data not shown). This suggests that AKK-mediated protection against *S.* Typhimurium could occur through a distinct mechanism from pAKK, and may involve the modulation of gut microbial metabolism.

AKK enhances the gut barrier and increases RegIII lectins secretion after infection

AKK and pAKK could plausibly influence several host intestinal functions which are critical for defense against *Salmonella* infection. First, we determined changes in gut barrier-related proteins after infection. Similar to our observations in uninfected mice, AKK-treated mice had higher levels of gene expression and increased tight junction proteins than pAKK or PBS-treated mice (Fig. 4A-F). We also directly visualized the distribution of tight junction proteins by immunofluorescence, and the results were consistent with RT-PCR and immunoblotting (Fig. 4G). We next examined the expression of lipocalin-2 (Lcn2), an innate immune protein and inflammatory marker. Oral administration of AKK

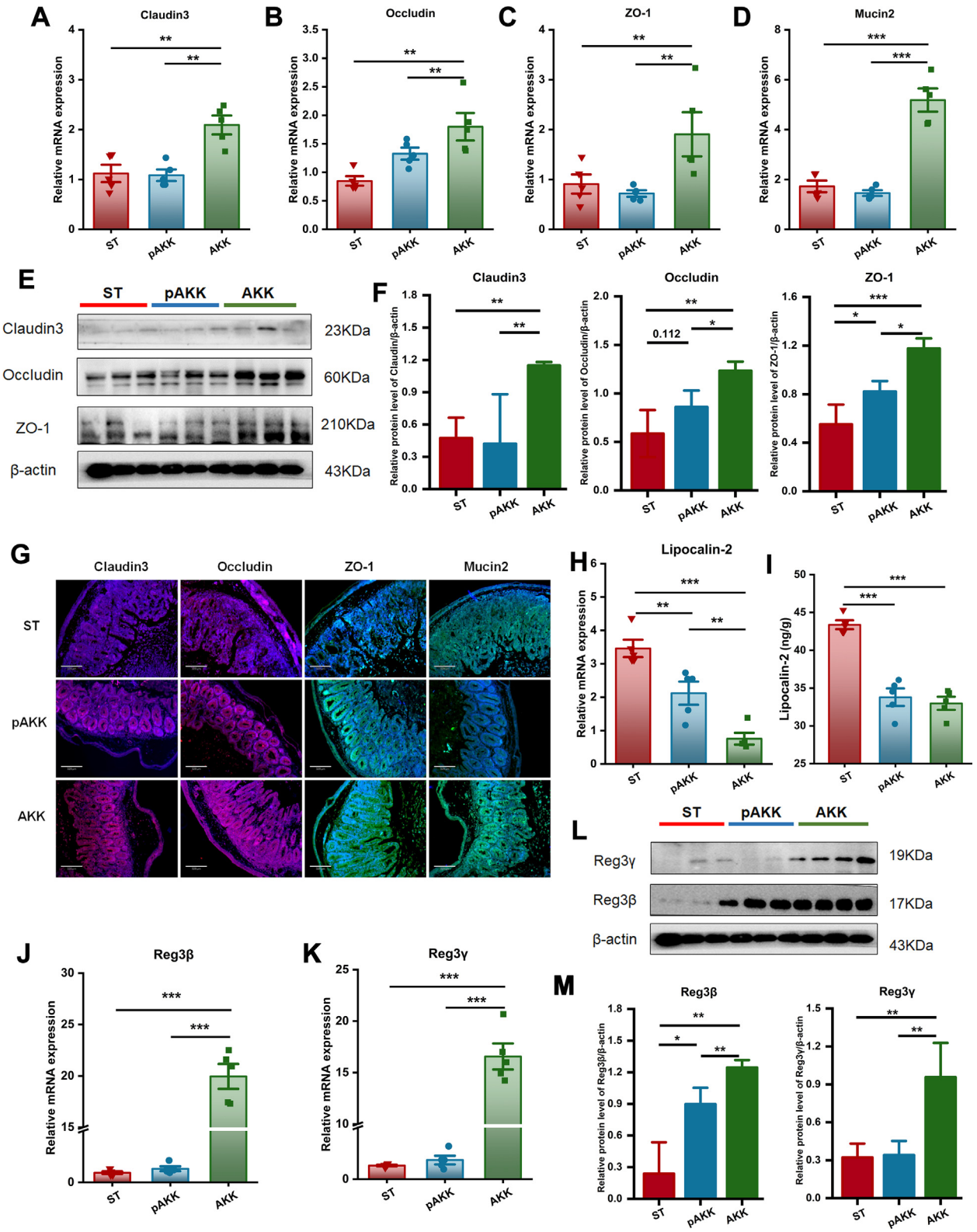

Fig. 4. Influence of AKK and pAKK on the expression of tight junction proteins and RegIII lectins in *Salmonella*-infected mice. The mRNA expression of (A) *Cldn3*, (B) *Ocln*, (C) *Tjp1*, and (D) *Muc2*. (E) Western blots for tight junction proteins. (F) Quantification of bands in E. (G) Immunofluorescence image of tight junction proteins. The blue color represents colonic cells stained with DAPI, the red color represents *Cldn3* and *Ocln* stained with Alexa Fluor 647, and the green color represents *Tjp1* and *Muc2* stained with Alexa Fluor 488. Images were taken at × 10 magnification. (H) The mRNA expression of Lcn2. (I) Lipocalin-2 levels determined by ELISA. The mRNA expression of (J) *Reg3b* and (K) *Reg3g*. (L) Western blots of RegIII proteins. (M) Quantification of bands in L. n = 3 ∼ 5. Statistical significance was determined by ANOVA for multiple comparisons and post-hoc Tukey test for comparisons between two groups. $^{*}p < 0.05$, $^{**}p < 0.01$, and $^{***}p < 0.001$. (For interpretation of the references to colour in this figure legend, the reader is referred to the web version of this article.)

and pAKK decreased Lcn2 expression in the cecum compared with PBS-treated mice (Fig. 4H and I). Since RegIII lectins are important for killing invading bacteria, we analyzed the expression of two members belonging to the RegIII family. We observed that AKK treatment strengthened transcript- and protein-level expression of Reg3β and Reg3γ in contrast to our observations in uninfected mice (Fig. 4J-M). As pAKK did not exert such broad effects on gut barrier function markers, these data indicate that AKK may specifically counteract *S.* Typhimurium pathogenesis by promoting the expression of tight junction proteins and antimicrobial RegIII lectins.

Pasteurized AKK activates NLRP3 and induces the expression of IL-1β.

To investigate whether AKK or pasteurized AKK was associated with inflammasome activation during the period of *S.* Typhimurium infection, we assessed the relative mRNA expression of NLRP3 and associated inflammatory caspases. TLR4, NLRP3, caspase-1and IL-1β were significantly upregulated in the cecum of pAKK-treated but not AKK-treated mice (Fig. 5A-D). Similar results were observed in protein expression (Fig. 5E and F), suggesting that in contrast to AKK's effects on gut barrier function, pAKK may instead selectively enhance inflammasome activity to augment host defense.

pAKK stimulates antimicrobial activity, ROS production, and inflammasome activation in macrophages

Beyond the effects on intestinal microbiota and gut barrier function, we hypothesized AKK and pAKK might play roles in host defense by stimulating the activity of innate immune cells such as tissue-resident macrophages. To test this hypothesis, RAW246.7 macrophages were pre-cultured with pAKK or AKK at different MOI for 24 h. No adverse effect was observed when MOI was lower than 10 (Fig. S3 A-D). Then, co-cultured cells were infected with *S.* Typhimurium SL1344 for 45 min, treated with gentamicin for 60 min, and plated on LB agar plates to count. Macrophages treated with pAKK and AKK resulted in lowered intracellular *S.* Typhimurium burdens, suggesting pAKK and AKK enhanced the antimicrobial function of macrophages (Fig. 6A and B). pAKK seemed to exert a stronger effect than AKK at the same MOI (Fig. 6C). Then we tested the effect of different treatment times on antimicrobial activity of macrophages, and found no significant difference was observed for pAKK (Fig. 6D). When the incubation time of macrophages extended from 60 min to 120 min, *S.* Typhimurium burdens in cell gradually decreased as the time increased (Fig. 6E). GFP-*Salmonella* was used to visualize the *S.* Typhimurium burdens in cell, we observed decreased fluorescence intensity in pAKK- or AKK- treated macrophages (Fig. 6F-6G).

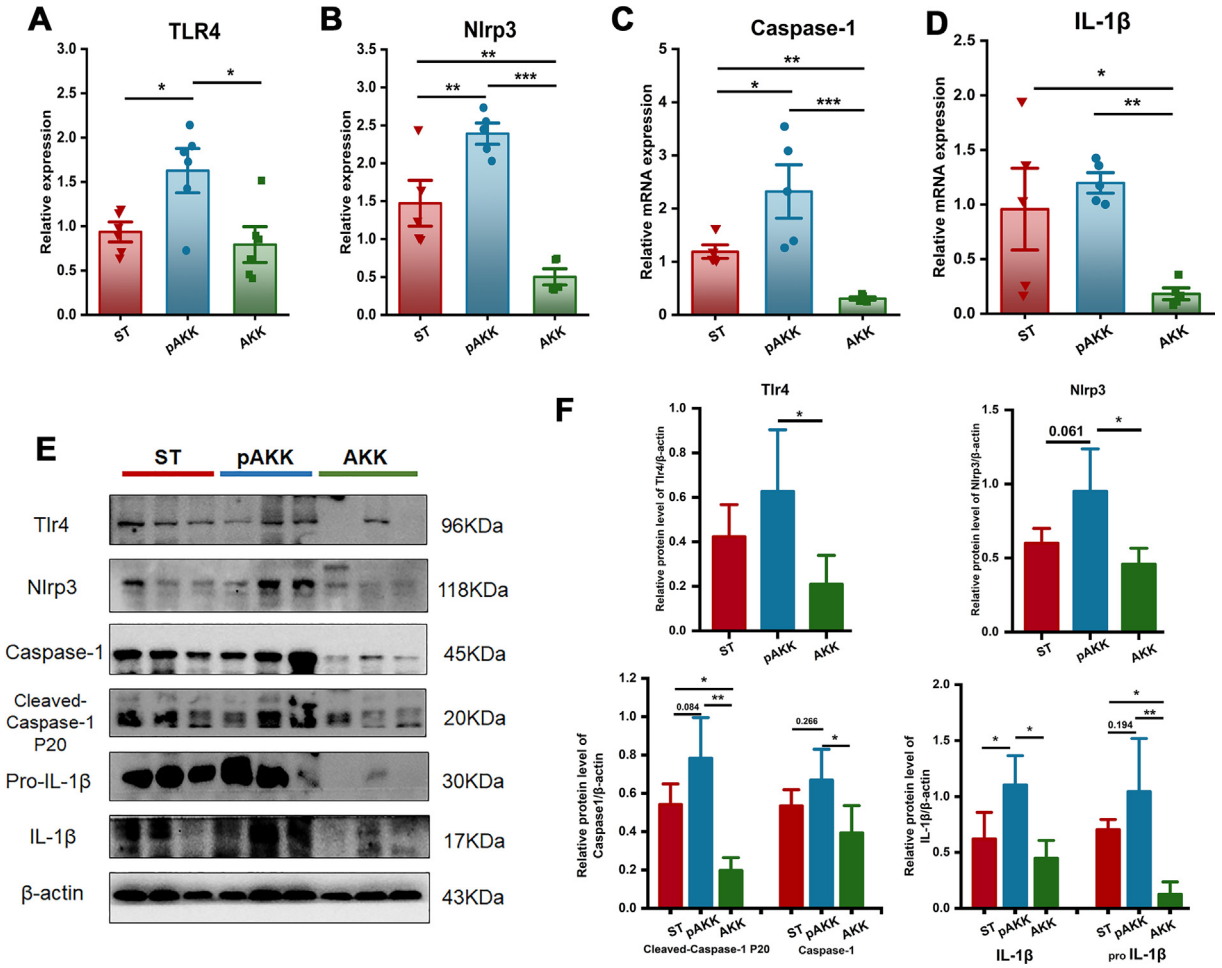

Fig. 5. Effect of AKK and pAKK on inflammasome expression and production of caspase-1 and IL-1β in infected mice. The mRNA expression of (A) TLR4, (B) NLRP3, (C) Caspase-1, and (D) IL-1β. (E) Western blots of inflammasome-related proteins. (F) Quantification of bands in E. n = 3 ∼ 5. Statistical significance was determined by ANOVA for multiple comparisons and post-hoc Tukey test for comparisons between two groups. $^{*}p < 0.05$, $^{**}p < 0$ 0.01, and $^{***}p < 0.001$.

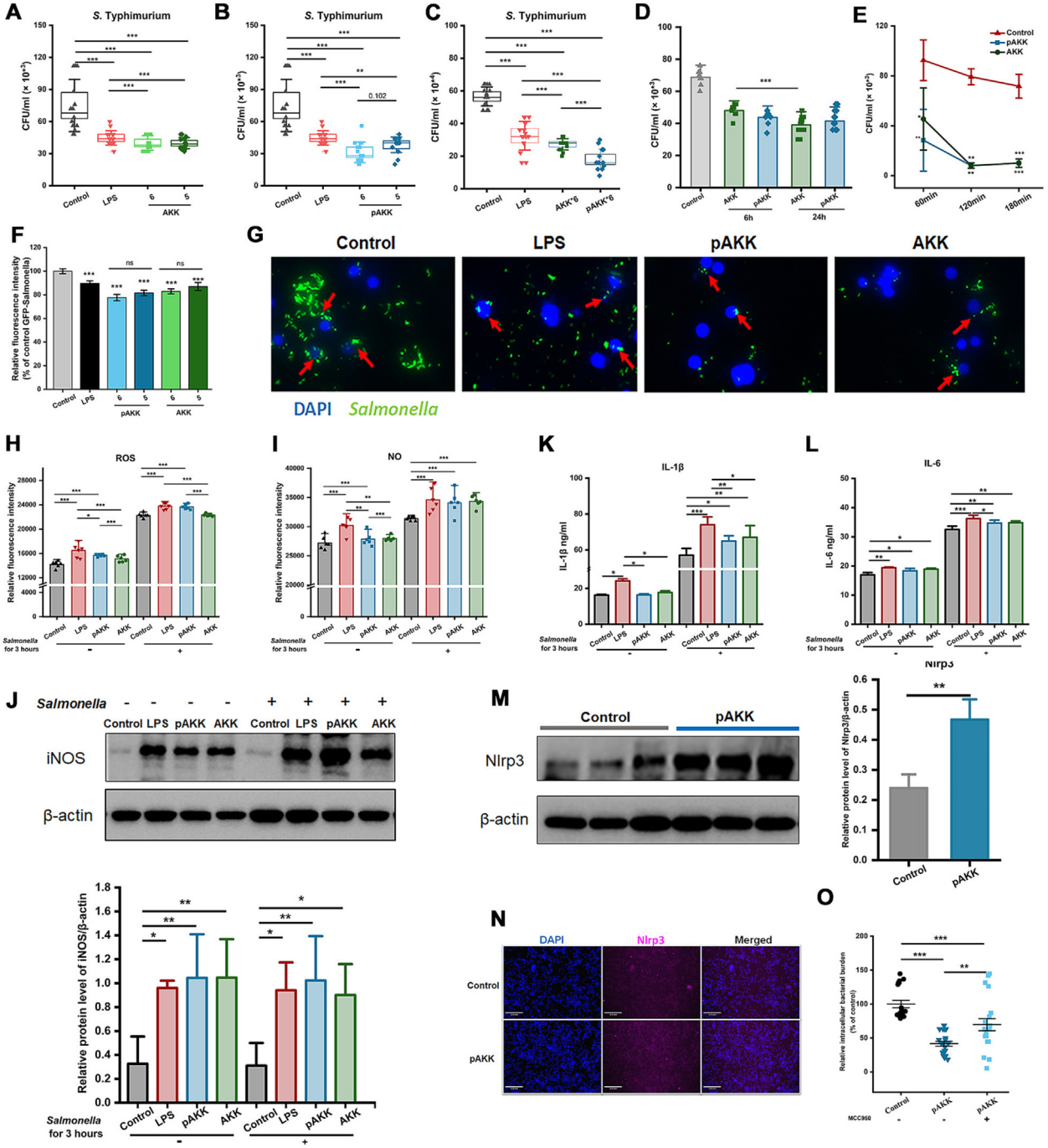

Fig. 6. Effect of AKK and pAKK on antimicrobial activity of macrophage and its NO and ROS production. The numbers of intracellular *Salmonella* in macrophages pretreated with (A) pAKK at different MOI for 24 h, (B) AKK at different MOI for 24 h, (C) pAKK or AKK at the same MOI for 24 h, and (D) pAKK or AKK at an MOI of 10 for 6 h or 24 h. (E) The antimicrobial kinetics of macrophages. (F) The fluorescence intensity of GFP-*S.* Typhimurium SL1314. (G) Representative image of GFP-*S.* Typhimurium. (H-N) Macrophages were pretreated with pAKK or AKK for 24 h, then infected with *S.* Typhimurium SL1314 for 3 h. After that, (H) ROS, (I) NO, (K) IL-1β, and (L) IL-6 were measured. (J) Western blotting (up) and band quantification (down) of iNOS. (M) Western blotting (left) and band quantification (right) of NLRP3. (N) Immunofluorescence image of NLRP3. (O) The number of intracellular *Salmonella* in macrophages pretreated with MCC950 for 24 h before pAKK treatment. Statistical significance was determined by ANOVA for multiple comparisons and post-hoc Tukey test for comparisons between two groups.$^{*}p < 0.05$, $^{**}p < 0.01$, and $^{***}p < 0.001$.

To test whether the exposure to AKK or pAKK altered the phagocytosis capacity of macrophages and reduces *Salmonella* uptake, we determined the phagocytosis rates and bacterial uptake using 0.9% of neutral red and GFP-*Salmonella* respectively. Our results showed phagocytosis capacity markedly increased after treatment in comparison to the control (Fig. S3E and F). The apoptosis of cells between control and pAKK group was similar, indicating cell death was not the cause of increased antimicrobial activity (Fig. S3G and H). Intestinal macrophages can respond to intracellular bacteria by producing factors such as ROS, NO, cytokines, and antimicrobial peptides [30]. pAKK or AKK-treated macrophages produced more ROS and NO than untreated macrophages in both steady-state or infection conditions (Fig. 6H and I). Consistent with increased NO production, the primary NO synthetic enzyme,

inducible NO synthase (iNOS) was upregulated in treated cells (Fig. 6J). Meanwhile, we also found that pAKK and AKK increased the level of IL-1β and IL-6 (Fig. 6K and L).

One host factor that could connect increased ROS production to inflammatory cytokine release is the activation of the NLRP3 inflammasome [31]. As we found a higher level of NLRP3 expression in pAKK-treated mice (Fig. 5), then we treated macrophages with pAKK for 24 h, and found a higher NLRP3 expression in comparison with the untreated macrophages (Fig. 6M and N). The enhanced antimicrobial activity of macrophages induced by pAKK was partly abolished by NLRP3 inhibitor MCC950, suggesting pAKK stimulation of antimicrobial activity is partly NLRP3-dependent.

AKK-altered gut microbiota play an important role in attenuating infection

To investigate whether the protective effects of AKK are in part mediated by gut microbiome, AKK-treated mice and naïve mice were co-housed for 2 weeks for natural microbiota transfer, then all mice were challenged with *S.* Typhimurium as mentioned

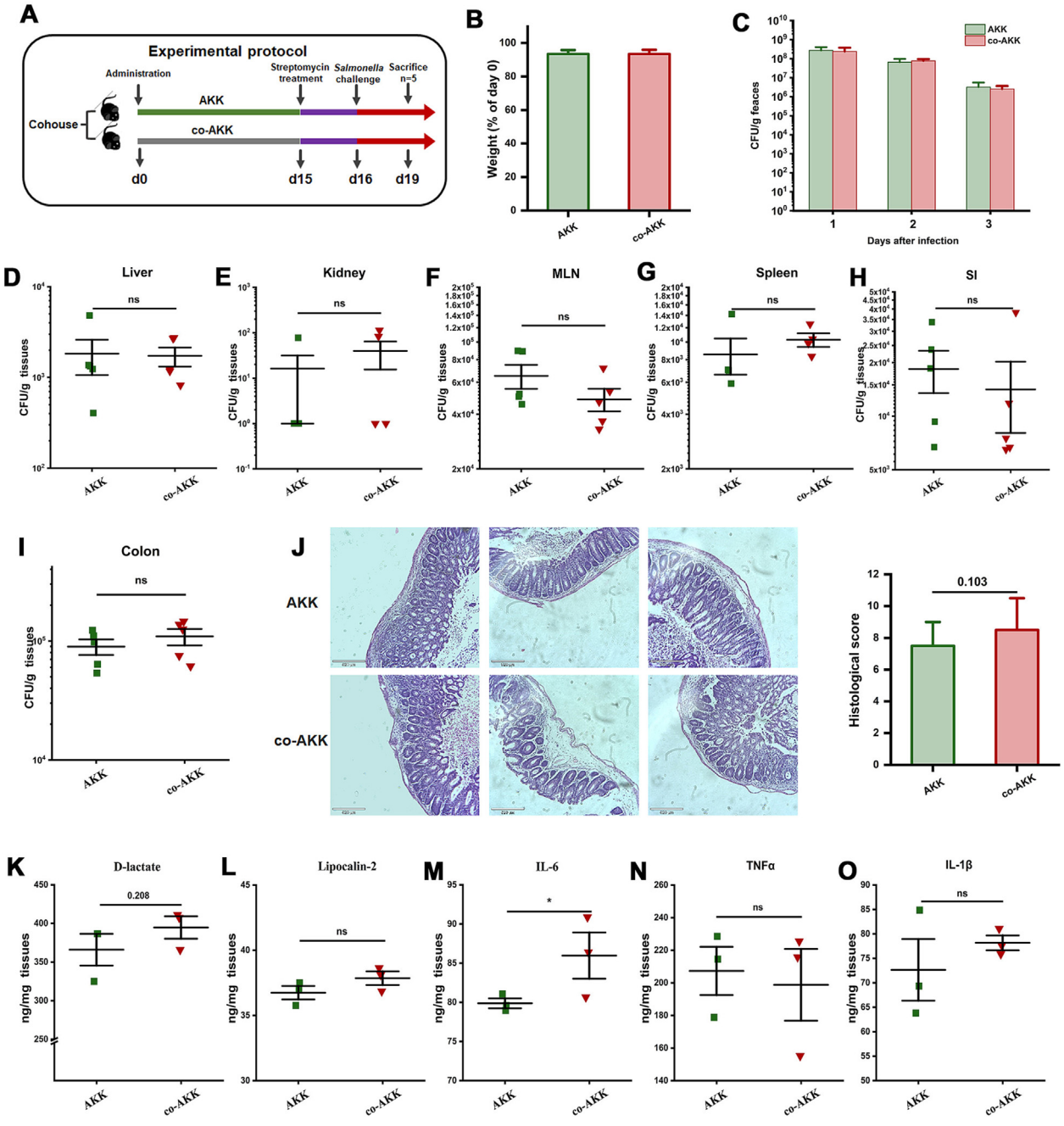

Fig. 7. The protective effect of AKK was transferable through gut microbiota to co-housed naïve mice. (A) Experimental design. Naïve mice (co-AKK) were co-housed with AKK-treated mice (AKK) for 14 days, then all mice were orally gavaged with streptomycin before challenging with 10^7 CFU/100 μL of *S.* Typhimurium SL1344. (B) Weight loss. (C) *S.* Typhimurium shedding in feces throughout the infection. *S.* Typhimurium burdens in tissues, including (D) liver, (E) kidney, (F) MLN, (g) spleen, (H) SI, (I) colon, n = 5. (J) Representative H&E stained cecal sections of mice (left) and histopathological scores (right). Images were taken at × 10 magnification. The cytokines production of (K) D-lactate in serum, (L) Lipocalin-2, (M) IL-6, (N) TNF-α, and (O) IL-1β in cecum, n = 3. Statistical significance was determined by ANOVA for multiple comparisons and post-hoc Tukey test for comparisons between two groups. $^*p < 0.05$.

earlier (Fig. 7A). All mice started to lose body weight after infection, and weight change was the same among the two groups (Fig. 7B). Importantly, naïve mice cohoused with AKK-treated mice showed no significant differences in *Salmonella* intestinal colonization or systemic dissemination (Fig. 7C-I) in contrast to AKK-treated mice. There was little difference between AKK-treated or cohoused naïve mice in histological inflammation scores or cecal cytokine levels, supporting the idea that co-housed naïve mice were protected similarly to AKK-treated mice (Fig. 7J-O). These data indicate that AKK-induced protective phenotype is transferrable and is at least partly mediated by gut microbiota.

Discussion

Since its discovery, *A. muciniphila* has now been recognized as an important mediator of host metabolism and immunity in several pathogenic contexts, and extensively studied for its health-promoting benefits including ameliorating metabolic disease and boosting immunotherapy [23,24]. However, in the setting of *Salmonella* infection, the role of *A. muciniphila* is not precisely known. Here we investigated the role of *A. muciniphila* during the infection induced by *S.* Typhimurium. We found both live and pasteurized *A. muciniphila* significantly reduced *S.* Typhimurium intestinal expansion, systemic colonization, and disease severity in mice. Profiling the host response to AKK and pAKK revealed distinctive candidate pathways of protective effects, with AKK likely enhancing gut barrier function, and pAKK likely promoting inflammasome activation and cytokines production.

The mucin constantly replenished by goblet cells, is highly glycosylated and linked proteins, which create a viscous hydrogel to protect the intestinal epithelium from resident microorganisms [32]. A fortified mucin layer could reduce bacteria motility and trap them in mucus meshwork. Meanwhile, an earlier study reported that accelerated mucin turnover was beneficial for clearing the invading bacteria when infected [33]. Mucin 2-deficient mice are highly susceptible to intestinal infection, indicating mucus layer plays a crucial role in defending against enteric pathogens [34]. *A. muciniphila* could restore gut barrier function and improve the mucin secretion of goblet cells in metabolic disorders or DSS-induced colitis [35]. High expression of Mucin 2 or other tight-junction protein was observed before and after infection in AKK-treated mice. This observation is consistent with *A. muciniphila*'s known function as a mucin-degrading bacterium, which can remodel the mucus layer in the intestine and stimulate mucus production of goblet cells. This supports the notion that AKK prevents infection partially from the improved gut barrier function.

AMPs produced by these host cells, such as RegIII lectins, are innate immune effectors in recognizing and killing invasive bacteria [36,37]. RegIII lectins could bind glycans like Mucin 2, making it easy to bind pathogen lipopolysaccharides, strengthen the mucus layer function, and exert its bactericidal action [38]. Before infection, Reg3β and Reg3γ expression were not significantly altered by AKK or pAKK treatment, while were both strongly induced after the *S.* Typhimurium challenge in AKK-treated mice. Therefore, the effects that we observed on barrier gene expression and RegIII production in AKK-treated mice may synergistically promote host defense.

A likely mechanism of colonization resistance has been linked to enhanced SCFAs production by the gut microbiota. SCFAs could limit pathogen expansion in several ways, including effects on intracellular pH, virulence gene expression, and stimulation of macrophage phagocytosis [30,39,40]. SCFAs, such as acetate and propionate, were significantly induced by AKK and pAKK treatment before infection, while propionate was only higher in feces of AKK-treated mice after infection. Meanwhile, *Bifidobacteriaceae* and *Bacteroidetes* were relatively enriched in AKK group before or after antibiotic treatment. Traditional probiotics, such as *Bifidobacterium*, have previously been linked to increased production of SCFAs [41]. In another study, *Bacteroidetes* provide colonization resistance against *S.* Typhimurium by the production of high-level propionate, indicating the role of specific microbial species in mediating pathogen resistance [28]. It is therefore plausible that *A. muciniphila* may support host defense through a similar mechanism.

Administration of both AKK and pAkk influenced the composition of the gut microbiota, and co-housing experiment indicated that microbial community transfer from AKK-treated mice might provide a protective effect on infection. Similarly, the mice received resistant communities during the cohousing reversed the susceptibilities to *C. rodentium* infection,[42]. These findings suggest that gut microbiota is likely indispensable to providing resistance in the host against infection.

A previous report has indicated *A. muciniphila* exacerbated the infection of *Salmonella* in germ-free mice with SIHUMI [25]. The difference between microbial community composition and mouse infection conditions could account for the opposing phenotypes we observed. The idea that a single commensal like *A. muciniphila* could divergently impact infection outcomes by the same pathogen depending on microbial and host context require further study, and future investigations should clarify the conditions where *A. muciniphila* is most likely to provide protection and act as a candidate probiotic. Though pAKK did not affect the expression of barrier genes or RegIII family members, we found that it might influence TLR-mediated regulation of the NLRP3 inflammasome in immune cells. Previous studies have verified that inflammasomes are required in response to the infection induced by pathogens, viruses, and parasites [5,7,31,43]. A key function of inflammasome activation is the stimulation of host cell death by apoptosis and pyroptosis, which in some cases constitutes a host defense strategy to restrict the replication and survival of pathogenic bacteria [44,45]. NLRP3 as a member of the NLR family activates the expression of caspase-1 and IL-1β when it is achieved by downstream activation of caspase-1, which induces the release of IL-1β and eventually causes host cell death [5,46,47]. NLRP3 deficiency exacerbates infection induced by pathogenic microorganisms, such as bacteria, viruses, and fungi [5,7,31]. *Akkermansia* supplementation increased the expression of NLRP3 in a DSS colitis model [48], similarly in this study pAKK treatment upregulated the NLRP3, and we found antimicrobial activity in macrophage decreased when NLRP3 was pharmacologically inhibited. Together, our data suggest that the protective phenotype caused by pAKK could be due to the enhancement of antimicrobial NO and ROS production as well as the regulation of cytokine levels.

Conclusion

In conclusion, we demonstrate that both live and pasteurized forms of *A. muciniphila* could alleviate *Salmonella* infection in mice. Live *A. muciniphila* plays an important role in regulation of intestinal microbial communities to decrease the dissemination of *Salmonella* via enhancing the intestinal barrier, promoting the expression of RegIII lectins, and producing SCFAs. Pasteurized *A. muciniphila* might activate the expression of NLRP3 and IL-1β as well as enhance NO and ROS production in macrophages to protect mice from *Salmonella* infection. The limitation of this study is that it remains undetermined which components or metabolites could mainly account for the beneficial effects induced by *A. muciniphila*. Detailed cell component analysis and metabolomic analysis are necessitated to pinpoint the main active substances and to decipher more potential mechanisms in future studies.

CRediT authorship contribution statement

Jiaxiu Liu: Visualization, Formal analysis, Methodology, Software, Writing – original draft, Writing – review & editing. **Hongli Liu:** Methodology, Software. **Huanhuan Liu:** Investigation, Methodology. **Yue Teng:** Investigation, Methodology. **Ningbo Qin:** Conceptualization, Validation. **Xiaomeng Ren:** Validation. **Xiaodong Xia:** Conceptualization, Supervision, Funding acquisition, Writing – review & editing.

Declaration of Competing Interest

The authors declare that they have no known competing financial interests or personal relationships that could have appeared to influence the work reported in this paper.

Acknowledgements

This work was supported partly by the National Key Research and Development Program of China (2022YFD2100104), and the Science and Technology Research Program of the Liaoning Department of Education (J2020044).

Appendix A. Supplementary data

Supplementary data to this article can be found online at https://doi.org/10.1016/j.jare.2023.03.008.

References

[1] Vieira K, Silva H, Rocha I, Barboza E, Eller L. Foodborne pathogens in the omics era. Crit Rev Food Sci Nutr 2021;1–16.
[2] Bahramianfard H, Derakhshandeh A, Naziri Z, Khaltabadi Farahani R. Prevalence, virulence factor and antimicrobial resistance analysis of *Salmonella Enteritidis* from poultry and egg samples in Iran. BMC Vet Res 2021;17(1):196.
[3] Sellin ME, Müller AA, Felmy B, Dolowschiak T, Diard M, Tardivel A, et al. Epithelium-intrinsic NAIP/NLRC4 inflammasome drives infected enterocyte expulsion to restrict *Salmonella* replication in the intestinal mucosa. Cell Host Microbe 2014;16(2):237–48.
[4] Muruve DA, Pétrilli V, Zaiss AK, White LR, Clark SA, Ross PJ, et al. The inflammasome recognizes cytosolic microbial and host DNA and triggers an innate immune response. Nature 2008;452(7183):103–7.
[5] Broz P, Newton K, Lamkanfi M, Mariathasan S, Dixit V, Monack D. Redundant roles for inflammasome receptors NLRP3 and NLRC4 in host defense against *Salmonella*. J Exp Med 2010;207(8):1745–55.
[6] Kamada AJ, Pontillo A, Guimarães RL, Loureiro P, Crovella S, Brandão LA. NLRP3 polymorphism is associated with protection against human T-lymphotropic virus 1 infection. Mem Inst Oswaldo Cruz 2014;109(7):960–3.
[7] Alhallaf R, Agha Z, Miller C, Robertson A, Sotillo J, Croese J, et al. The NLRP3 Inflammasome Suppresses Protective Immunity to Gastrointestinal Helminth Infection. Cell Rep 2018;23(4):1085–98.
[8] Mullineaux-Sanders C, Suez J, Elinav E, Frankel G. Sieving through gut models of colonization resistance. Nat Microbiol 2018;3(2):132–40.
[9] Rogers AWL, Tsolis RM, Bäumler AJ. *Salmonella* versus the Microbiome. Microbiol Mol Biol Rev 2021;85(1):e00027–119.
[10] Chassaing B, Cascales E. Antibacterial Weapons: Targeted Destruction in the Microbiota. Trends Microbiol 2018;26(4):329–38.
[11] Leshem A, Liwinski T, Elinav E. Immune-Microbiota Interplay and Colonization Resistance in Infection. Mol Cell 2020;78(4):597–613.
[12] Buffie CG, Bucci V, Stein RR, McKenney PT, Ling L, Gobourne A, et al. Precision microbiome reconstitution restores bile acid mediated resistance to *Clostridium difficile*. Nature 2015;517(7533):205–8.
[13] Sorbara M, Dubin K, Littmann E, Moody T, Fontana E, Seok R, et al. Inhibiting antibiotic-resistant *Enterobacteriaceae* by microbiota-mediated intracellular acidification. J Exp Med 2019;216(1):84–98.
[14] Pedicord VA, Lockhart AAK, Rangan KJ, Craig JW, Loschko J, Rogoz A, et al. Exploiting a host-commensal interaction to promote intestinal barrier function and enteric pathogen tolerance. Sci Immunol 2016;1(3):eaai7732.
[15] Derrien M, van Passel M, van de Bovenkamp J, Schipper R, de Vos W, Dekker J. Mucin-bacterial interactions in the human oral cavity and digestive tract. Gut Microbes 2010;1(4):254–68.
[16] Depommier C, Van Hul M, Everard A, Delzenne N, De Vos W, Cani P. Pasteurized increases whole-body energy expenditure and fecal energy excretion in diet-induced obese mice. Gut Microbes 2020;11(5):1231–45.
[17] Wang L, Tang L, Feng Y, Zhao S, Han M, Zhang C, et al. A purified membrane protein from or the pasteurised bacterium blunts colitis associated tumourigenesis by modulation of CD8 T cells in mice. Gut 2020;69(11):1988–97.
[18] Everard A, Belzer C, Geurts L, Ouwerkerk JP, Druart C, Bindels LB, et al. Cross-talk between *Akkermansia muciniphila* and intestinal epithelium controls diet-induced obesity. Proc Natl Acad Sci U S A 2013;110(22):9066–71.
[19] Zhao S, Liu W, Wang J, Shi J, Sun Y, Wang W, et al. *Akkermansia muciniphila* improves metabolic profiles by reducing inflammation in chow diet-fed mice. J Mol Endocrinol 2017;58(1):1–14.
[20] Plovier H, Everard A, Druart C, Depommier C, Van Hul M, Geurts L, et al. A purified membrane protein from *Akkermansia muciniphila* or the pasteurized bacterium improves metabolism in obese and diabetic mice. Nat Med 2017;23(1):107–13.
[21] Qian K, Chen S, Wang J, Sheng K, Wang Y, Zhang M. A β-N-acetylhexosaminidase Amuc_2109 from *Akkermansia muciniphila* protects against dextran sulfate sodium-induced colitis in mice by enhancing intestinal barrier and modulating gut microbiota. Food Funct 2022;13(4):2216–27.
[22] Jiang Y., Y. Xu, C. Zheng, L. Ye, P. Jiang, S. Malik, G. Xu, Q. Zhou and M. Zhang. Acetyltransferase from *Akkermansia muciniphila* blunts colorectal tumourigenesis by reprogramming tumour microenvironment. Gut. 2023: gutjnl-2022-327853.
[23] Yoon H, Cho C, Yun M, Jang S, You H, Kim J, et al. *Akkermansia muciniphila* secretes a glucagon-like peptide-1-inducing protein that improves glucose homeostasis and ameliorates metabolic disease in mice. Nat Microbiol 2021;6(5):563–73.
[24] Bae M, Cassilly CD, Liu X, Park SM, Tusi BK, Chen X, et al. *Akkermansia muciniphila* phospholipid induces homeostatic immune responses. Nature 2022;608(7921):168–73.
[25] Ganesh B, Klopfleisch R, Loh G, Blaut M. Commensal *Akkermansia muciniphila* exacerbates gut inflammation in *Salmonella* Typhimurium-infected gnotobiotic mice. PLoS One 2013;8(9):e74963.
[26] Mao T, Su C, Ji Q, Chen C, Wang R, Vijaya Kumar D, et al. Hyaluronan-induced alterations of the gut microbiome protects mice against *Citrobacter rodentium* infection and intestinal inflammation. Gut Microbes 2021;13(1):1972757.
[27] Derrien M, Vaughan EE, Plugge CM, de Vos WM. *Akkermansia muciniphila* gen. nov., sp. nov., a human intestinal mucin-degrading bacterium. Int J Syst Evol Microbiol 2004;54(Pt 5):1469–76.
[28] Jacobson A, Lam L, Rajendram M, Tamburini F, Honeycutt J, Pham T, et al. A gut commensal-produced metabolite mediates colonization resistance to *Salmonella* infection. Cell Host Microbe 2018;24(2):296–307.e7.
[29] Stecher B, Hardt WD. The role of microbiota in infectious disease. Trends Microbiol 2008;16(3):107–14.
[30] Smythies LE, Sellers M, Clements RH, Mosteller-Barnum M, Meng G, Benjamin WH, et al. Human intestinal macrophages display profound inflammatory anergy despite avid phagocytic and bacteriocidal activity. J Clin Invest 2005;115(1):66–75.
[31] Hise A, Tomalka J, Ganesan S, Patel K, Hall B, Brown G, et al. An essential role for the NLRP3 inflammasome in host defense against the human fungal pathogen *Candida albicans*. Cell Host Microbe 2009;5(5):487–97.
[32] Furter M, Sellin ME, Hansson GC, Hardt WD. Mucus Architecture and Near-Surface Swimming Affect Distinct *Salmonella* Typhimurium Infection Patterns along the Murine Intestinal Tract. Cell Rep 2019;27(9):2665–2678.e3.
[33] McLoughlin K, Schluter J, Rakoff-Nahoum S, Smith AL, Foster KR. Host Selection of Microbiota via Differential Adhesion. Cell Host Microbe 2016;19(4):550–9.
[34] Van der Sluis M, De Koning BA, De Bruijn AC, Velcich A, Meijerink JP, Van Goudoever JB, et al. Muc2-deficient mice spontaneously develop colitis, indicating that MUC2 is critical for colonic protection. Gastroenterology 2006;131(1):117–29.
[35] Cani PD, Depommier C, Derrien M, Everard A, de Vos WM. *Akkermansia muciniphila*: paradigm for next-generation beneficial microorganisms. Nat Rev Gastroenterol Hepatol 2022;19(10):625–37.
[36] van Ampting M, Loonen L, Schonewille A, Konings I, Vink C, Iovanna J, et al. Intestinally secreted C-type lectin Reg3b attenuates salmonellosis but not listeriosis in mice. Infect Immun 2012;80(3):1115–20.
[37] Loonen LM, Stolte EH, Jaklofsky MT, Meijerink M, Dekker J, van Baarlen P, et al. REG3γ-deficient mice have altered mucus distribution and increased mucosal inflammatory responses to the microbiota and enteric pathogens in the ileum. Mucosal Immunol 2014;7(4):939–47.
[38] Miki T, Okada N, Hardt W. Inflammatory bactericidal lectin RegIIIβ: Friend or foe for the host? Gut Microbes 2018;9(2):179–87.
[39] Wu T, Li H, Su C, Xu F, Yang G, Sun K, et al. Microbiota-Derived Short-Chain Fatty Acids Promote LAMTOR2-Mediated Immune Responses in Macrophages. mSystems 2020;5(6):e00587–620.
[40] Liu J, Zhu W, Qin N, Ren X, Xia X. Propionate and Butyrate Inhibit Biofilm Formation of *Salmonella* Typhimurium Grown in Laboratory Media and Food Models. Foods 2022;11(21):3493.
[41] O'Toole PW, Marchesi JR, Hill C. Next-generation probiotics: the spectrum from probiotics to live biotherapeutics. Nat Microbiol 2017;2:17057.
[42] Osbelt L, Thiemann S, Smit N, Lesker T, Schröter M, Gálvez E, et al. Variations in microbiota composition of laboratory mice influence *Citrobacter rodentium* infection via variable short-chain fatty acid production. PLoS Pathog 2020;16(3):e1008448.
[43] Burgueño J, Abreu M. Epithelial Toll-like receptors and their role in gut homeostasis and disease. Nat Rev Gastroenterol Hepatol 2020;17(5):263–78.

[44] Jorgensen I, Miao E. Pyroptotic cell death defends against intracellular pathogens. Immunol Rev 2015;265(1):130–42.
[45] Tummers B, Mari L, Guy C, Heckmann B, Rodriguez D, Rühl S, et al. Caspase-8-Dependent Inflammatory Responses Are Controlled by Its Adaptor, FADD, and Necroptosis. Immunity 2020;52(6):994–1006.e8.
[46] Crowley SM, Han X, Allaire JM, Stahl M, Rauch I, Knodler LA, et al. Intestinal restriction of *Salmonella* Typhimurium requires caspase-1 and caspase-11 epithelial intrinsic inflammasomes. PLoS Pathog 2020;16(4):e1008498.
[47] Knodler LA, Crowley SM, Sham HP, Yang H, Wrande M, Ma C, et al. Noncanonical inflammasome activation of caspase-4/caspase-11 mediates epithelial defenses against enteric bacterial pathogens. Cell Host Microbe 2014;16(2):249–56.
[48] Qu S, Fan L, Qi Y, Xu C, Hu Y, Chen S, et al. *Akkermansia muciniphila* alleviates dextran sulfate sodium (DSS)-induced acute colitis by NLRP3 activation. Microbiol Spectr 2021;9(2):e0073021.